Submitted to Nanoscale

Supporting Information - The role of metal layers in the formation of metal/silicon hybrid nanoneedle arrays

Hai Liu[1], *Chee Ying Khoo*[1], *Boluo Yadian*[1], *Qing Liu*[1], *Chee Lip Gan*[1], *Xiaohong Tang*[2], *Yizhong Huang*[1,*]

Supplementary Data

1) A matrix of various metal-coated silicon substrates under rastering of gradually increased ion doses.

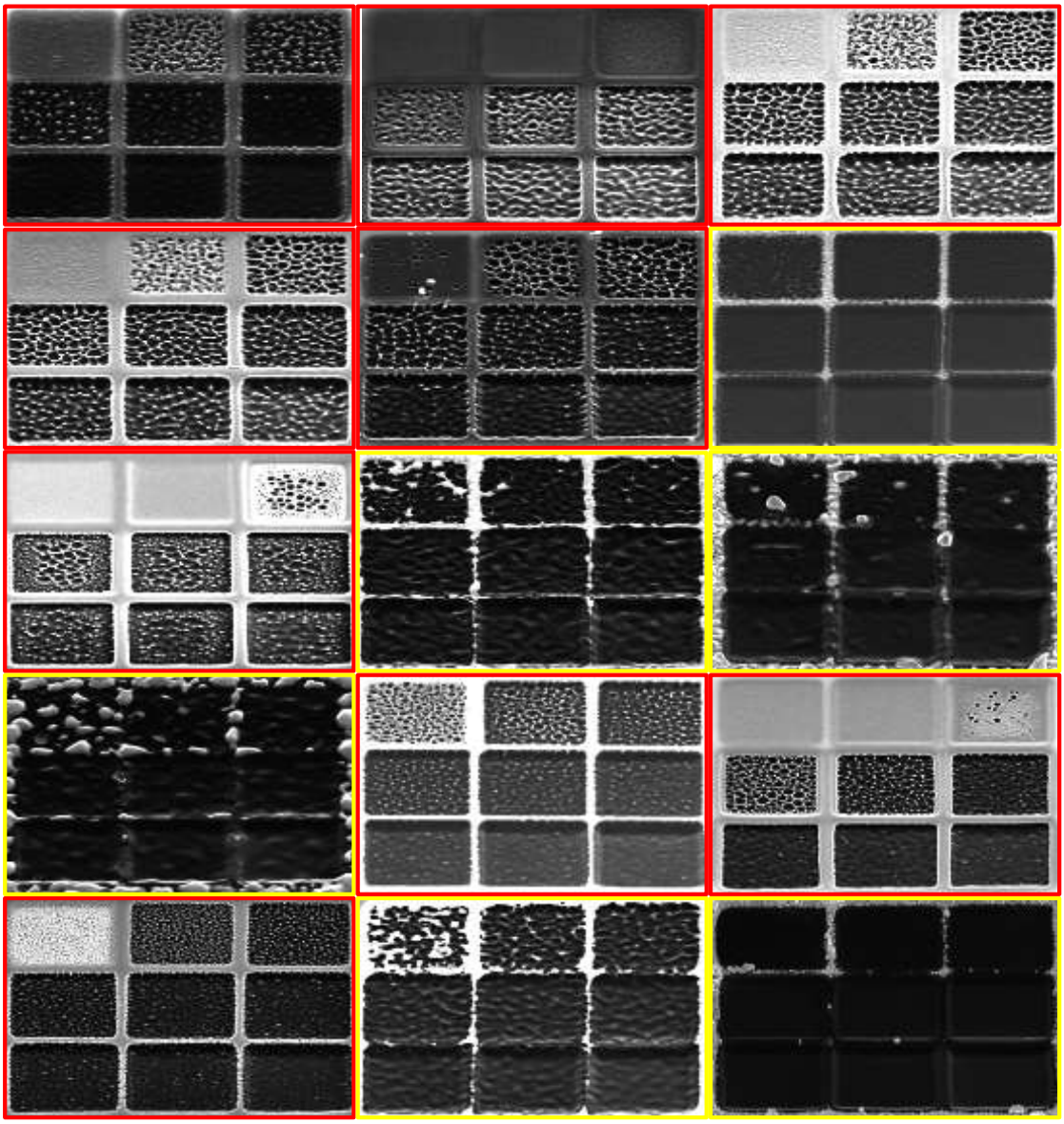

Fig. S1 A matrix of SEM images captured in an oblique angle of 52° showing gradually increasing ion dose to various metals coating on silicon substrate. Metal materials are arranged in the order of atom numbers, from left to right, top to bottom: Al, Ti, Cr, Fe, Co, Zn, Mo, Ag, In, Sn, Hf, Ta, W, Au and Bi.

There are nanodots formed on the surface red squared substrates with moderate ion dose, whilst the metallic layer suddenly removed on the other yellow ones. The topography of metal/silicon substrate after ion irradiation is quite correlated to their sputter rate/yield, as shown in the following table based theoretic calculation.

2) A sputter rate/yield table of metal under 30 keV Ga^+ irradiation.

Metal	Atomic number	Relative atomic mass	Sputter yield [1]	Sputter rate	Sputter yield[2-4]	Sputter rate
Al	13	27.0	1.290	0.134	1.476	0.153
Si	14	28.1	0.734	0.092	0.689	0.086
Ti	22	47.9	1.119	0.122	0.798	0.087
Cr	24	52	1.712	0.130	---	---
Fe	26	55.8	1.720	0.127	1.278	0.094
Co	27	58.9	1.715	0.118	1.998	0.138
Zn	30	65.4	20.392	1.942	---	---
Mo	42	95.9	1.195	0.117	1.279	0.125
Ag	47	108	7.255	0.773	4.982	0.531
In	49	115	---	---	---	---
Sn	50	119	7.015	1.185	---	---
Hf	72	178	2.617	0.364	1.495	0.208
Ta	73	181	1.694	0.191	---	---
W	74	184	1.420	0.141	1.044	0.104
Au	79	197	8.385	0.888	4.625	0.490
Bi	83	209	---	---	---	---

"---" : not available. Sputter yield in a unit of [atoms/ion] and sputter rate in a unit of [μm^3/nC].

The total sputter yield based on Sigmund theory from Ref [1] and Yamamura empirical formula from Ref [3, 4]. The corresponding sputter rate S_r can be induced from the sputter yield S_y by the equation shown as :

$$S_r = \frac{S_y \times 1.04 \times 10^{-14} \times M}{\rho} [\mu m^3 / nC]$$

where 1 nC incident beam contains 1.04×10^{-14}mol ions, to sputter of the material with atomic weight M [g/mol] and density ρ [g•µm-3] of the substrate. By the comparison between the matrix and table, it is quite obvious that the only the low-sputter-rate(yield)

metal can survive by forming nanodots with incident ions.

3) A matrix of various metal-coated silicon substrates after square mesh patterning.

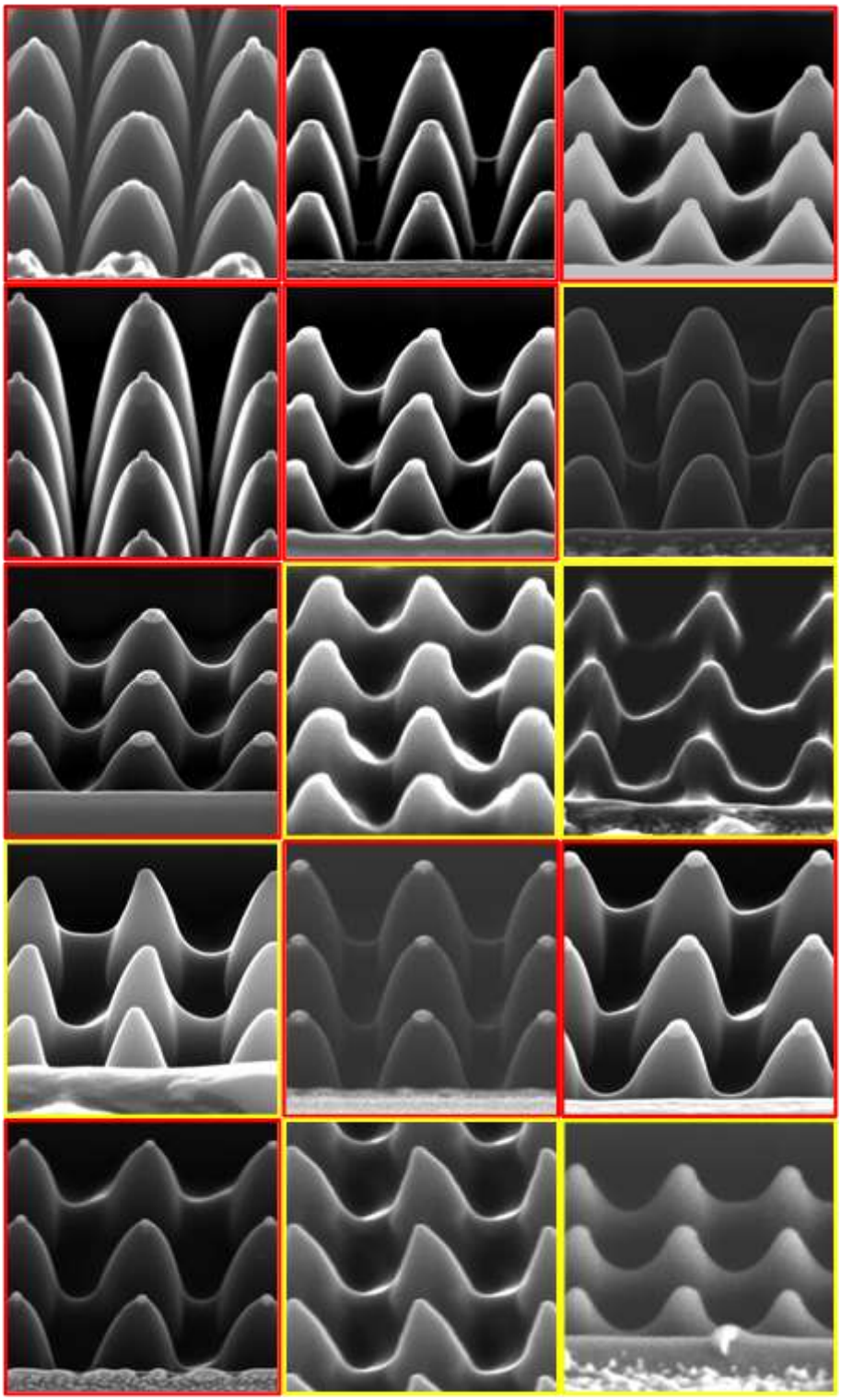

Fig. S2 SEM images viewed in an oblique angle of 52° showing the nanoneedles array patterned on various metals/silicon substrates. The distance of adjacent nanotip is ~700 nm. Metal materials are placed in the matrix with the same arrangement as Fig. S1, from left to right, top to bottom: Al, Ti, Cr, Fe, Co, Zn, Mo, Ag, In, Sn, Hf, Ta, W, Au and Bi.

It can be found that the low-sputter-rate metals, which can survive under medium ion dose rastering, can also result into the hybrid nanoneedle array under square mesh pattern. The microstructures of these metal/silicon hybrid nanoneedles are similar to that of chromium, as shown in Fig. S3.

4) Characterizations of selected metal/silicon hybrid nanoneedles compared to Cr/Si.

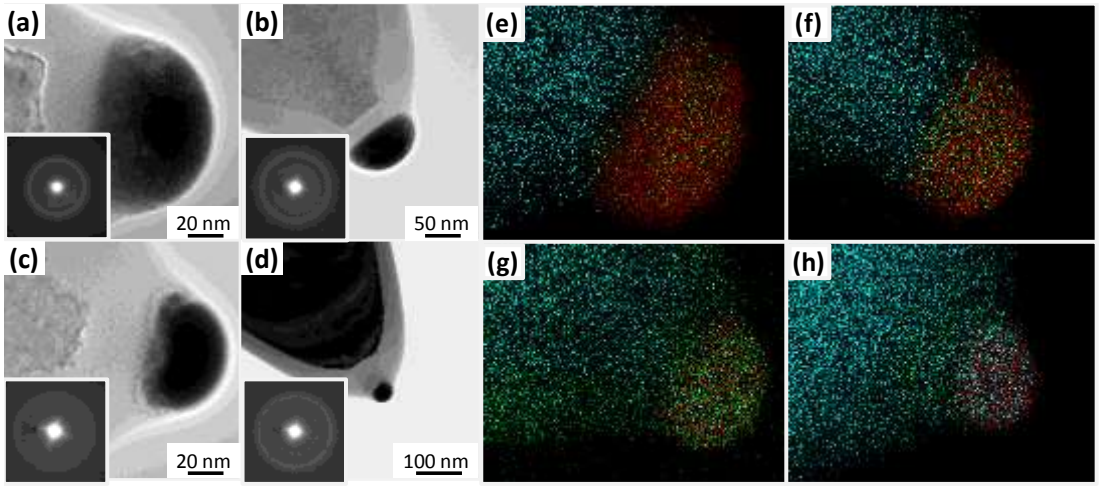

Fig. S3 Bright field TEM images and diffraction patterns (inset) from nanodots of the hybrid nanoneedles on substrate: (a) Cr/Si; (b) Co/Si; (c) Ta/Si; (d) W/Si. And the corresponding EDX elemental mappings (e-h), where cyan: silicon, green: gallium and red: (e) chromium, (f) cobalt, (g) tantalum and (h) tungsten.

The small difference of profile between nanoneedles may be caused by the different Ga irradiation during TEM sample preparation. Based on the TEM observation results, it is shown that the general microstructures originating from low-sputter-rate metals are quite similar to each other, in terms of an alloyed nanodot sitting on the top of a silicon nanoneedle.

5) Failed fabrication of hybrid nanoneedles by undesirable beam parameters.

The undesirable ion beam irradiation will cause the failure of hybrid nanoneedles array formation on a low-sputter-rate metal/silicon substrate. These ion beam parameters include: the low beam current (48 pA and 28 pA with much shorter tails in Fig S4 a and b), large space (1.5 μm in Fig. S4c) or small distance (300 nm in Fig. S4d) between the

adjacent nanoneedles. As the secondary electron images shown in Fig S4, all of them can not result in the formation of nanodot on top of each nanoneedle during ion milling.

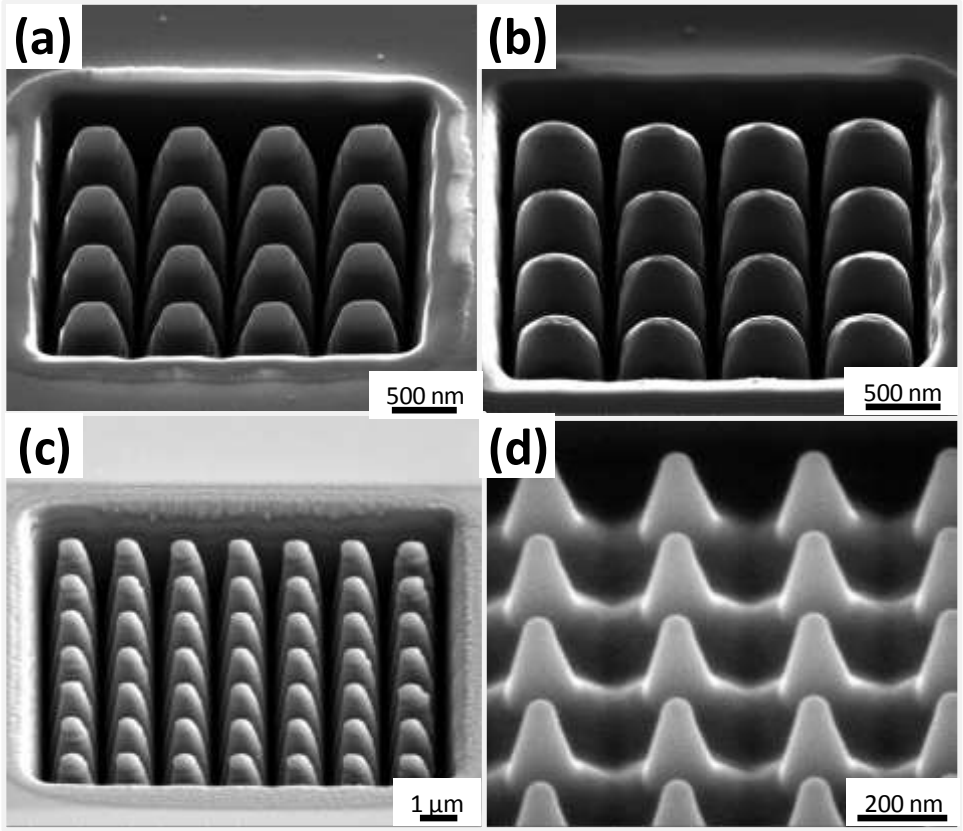

Fig.S4 Various failures of hybrid nanoneedles array fabrications on a Cr/Si substrate: (a) A 4 × 4 nanopillar array with a 700 nm space between adjacent nanoneedles. A long-term irradiation (10 min) provides sufficient ion dose to form such a small array of nanoneedles, but the low current (**48 pA**) with a much shorter tail is deficient for the Ga to alloy with the surface metal producing metallic nanodot. (b) The same pattern as (a) but at an even lower current of **28 pA**. After 20 minutes' irradiation, the much narrower beam tail induces the blunt nanorods of lower aspect ratio instead of nanoneedles. (c) A 7 × 7 nanoneedle array with a periodic separation of **1.5 µm** after 6 minutes of 2.8 nA ion patterning. The ions projected onto the nanotip (far from the beam center) are too weak to alloy with the Cr metal layer. (d) A magnified area within the 20 × 20 array under ion milling with current of 2.8 nA. In contrast to (c), the small periodic distance (**~300 nm**) results in the excessive ion dose in the beam tail. Only one minute is sufficient to remove the entire metallic layer without forming nanodots.

6) Evolution of catalytic Fe/Au/Si hybrid nanoneedles formation.

In order to verify the proposed hybrid nanoneedle formation mechanism, a series of Fe/Au/Si TEM samples are prepared and characterized in association with the individual stages illustrated in Fig. 3b-d. As shown in Fig. S5a, there are a couple of nanodots sitting on the bank of nanotrench with preliminary ion irradiation. An EDX elemental mapping of

Fig. S5b is taken from the square region where the iron shell is seen to be clearer in this stage than the final stage (Fig. 4c). With additional ion bombardment (Fig S5c), the coalescence of these two nanodots occurs on the tip of nanoneedle followed by fusion as indicated from a bright interface between them (see Fig. S5d). More ion irradiation results in the integration of two nanodots (Fig. S5e) leading to the formation of grain boundaries in the middle of nanodot (Fig. S5f).

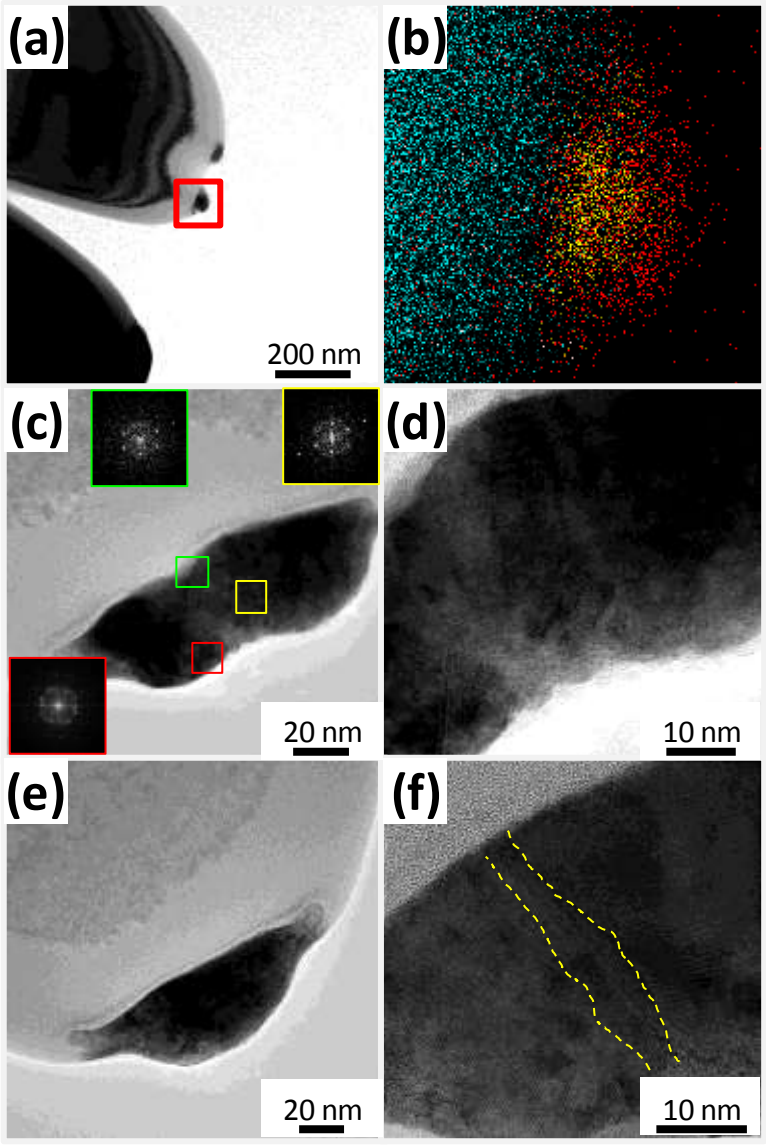

Fig.S5 A series of TEM images showing the evolution of Fe/Au/Si hybrid nanoneedles subjected to ion irradiation. (a) The alloy formed on the edge of nanotip, where the EDX elemental mapping (b) is taken from the square region (green: Ga, red: Fe, yellow: Au and cyan: Si). (c) The coalescence of nanodots on top of each nanoneedle. The inset FFT patterns are taken from the respective square region, which show their different orientations. (d) A magnified image showing that lattice of gold grains and their interface region in a bright contrast (merge insufficiently). (e) An integrated single nanodot

consisting of crystalline grains, confirmed by the HRTEM image in (f), where a couple of grain boundaries are visible (as highlighted in yellow lines).

References:

1 Orloff J, Utlaut M and Swanson L 2002 *High Resolution Focused Ion Beams: FIB and Its Applications* (New York: Kluwer Academic/Plenum Publishers) chapter 4, p 137

2 *www.asu.edu/clas/csss/NUE/FIBSputterCalcYamamura*

3 Y. Yamamura and H. Tawara *Atom Data Nucl. Data*, 1996, **62**, 149

4 Y. Yamamura *et al* IIPJ-AM-26, *Institute of Plasma Physics*, Nagoya University1983